FEM Analysis of the Load Distribution over the Face Width of Helical Gear Pairs Considering Deviations, Misalignments and Deformations

Prof. Dr. Eng. A. Mihailidis; Dipl. Eng. A. Psarros

Introduction

The load carrying capacity of spur gears may be calculated by ISO 6336 using influence factors. The face load factor $K_{H\beta}$ considers the impact of the non-uniform load distribution over the face width. Even if the gears had perfect geometry, the load would not distribute uniformly along the contact lines. The face load factor depends on deformations of all parts of the containing gearbox and mainly of the teeth, gears and shafts as well as on manufacturing and assembly deviations.

A nonlinear multi-point meshing model was developed by Zhou et al (Ref. 1) for determining the face load factor of spur gears. Multiple non-linear springs were used along the path of contact and rigid bars connected the gear with the shaft, which was modeled by beam elements. The process was iterative, and the results were compared with those obtained by finite element analysis (FEA). Roda-Casanova et al (Ref. 2) investigated the face load factor in straight spur gears, as calculated by ISO using finite elements. They considered the shaft diameter, misalignment and center distance errors, as well as the position of the gears on the shaft. Results were compared with ISO 6336. Yuan et al (Ref. 3) developed a coupled loaded tooth contact analysis (LTCA) model and a Timoshenko beam element model of spur and helical gears. Both static and dynamic cases were investigated and compared with a 3-D finite element approach. Four supporting layouts were chosen considering the power flow and the position of the bearings and the gears on the shafts. Results showed the contact

	Pinion	Gear
Number of teeth z	13	24
Addendum modification coefficient x	0.8	0.374
Tip diameter d_a [mm]	16.25	26.4
Module m [mm]	1	
Helix angle p [degrees]	0	
Centre distance a [mm]	19.5	
Face width b [mm]	15	
Bottom clearance c_p [mm]	0.25	
Basic rack	DIN 867	
Backlash [µm]	30	

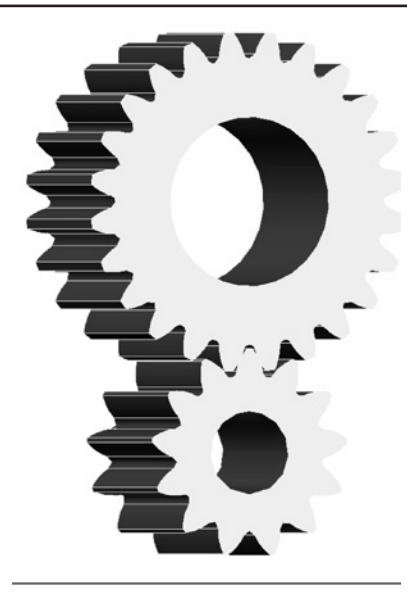

Figure 1 Gear data of the modeled spur gear.

	Pinion	Gear
Number of teeth z	13	24
Addendum modification coefficient x	0.8	0.757
Tip diameter d_a [mm]	16.85	28.65
Module m_n [mm]	1	
Helix angle p [degrees]	20	
Centre distance a [mm]	21	
Face width b [mm]	15	
Bottom clearance c_p [mm]	0.25	
Basic rack	DIN 867	
Backlash [µm]]	30	
Gear shaft diameter [mm]	6	15
haft length L [mm]	45	

Figure 2 Gear data and of the modeled helical gear pair.

This paper was first presented at International Conference on Gears 2019, 3rd International Conference on High Performance Plastic Gears 2019, 3rd International Conference on Gear Production 2019, Garching/Munich (VDI-Berichte 2355, 2019, VDI Verlag GmbH, Page 193–202.

pattern for each case and it was concluded that a torque increase results in stronger vibrations due to higher mesh misalignment.

Generally, two approaches are used for calculating the load distribution, based on multi-body dynamics and FEA. It is not only useful for validating the results — it also allows for much more detailed geometry modeling and therefore offers good accuracy. Custom numerical models have the advantage that they are in most cases solved in much less time.

In the current study, FEA is used. First, a simple model of contact between two parallel cylinders is made. Comparing the results obtained with those calculated following the well-known Hertzian theory, the mesh parameters and quality criteria are established. Next, a straight spur gear model is solved considering only the deformation of the teeth. After evaluating the results, a helical gear is modeled, considering again only the deformation of the teeth. Next, the deformation of the shafts is introduced and pitch errors imposed to the model. Gears remained in the same position in all above cases in order to directly compare the results.

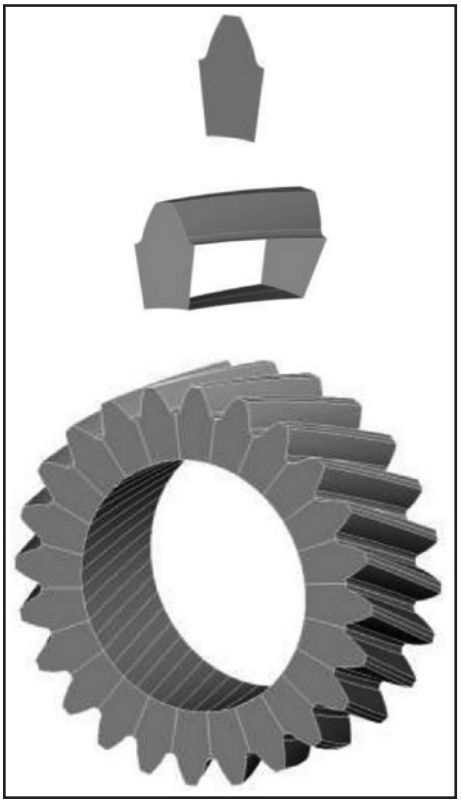

Figure 3 Generation of a 3-D helical gear model in three steps.

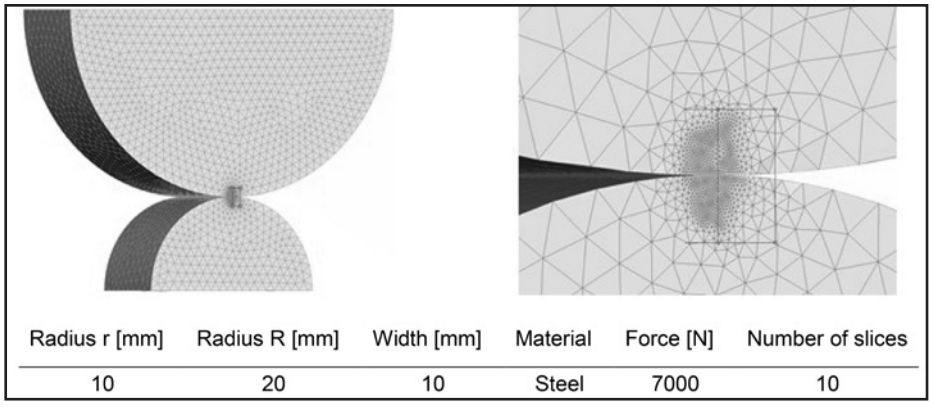

Figure 4 Hertzian contact model data and mesh.

Gear Pairs

In the current study two gears pairs are modeled. The first consists of a straight spur gear pair; its main data are shown (Fig. 1). The second gear pair consists of helical gears (Fig. 2). The impact of the deformation of the supporting shafts and the pitch errors of the active flanks are investigated for the more general case of helical gears. All gears have the same face width and they are made from case hardened steel. The gears are fixed in the center of their shafts.

Finite Element Modeling

Geometry generation. Modeling is carried out using the *ANSA* (Ref. 4) and *META* (Ref. 5) software of *BETA-CAE*. At first, a geometrically perfect 2-D gear tooth segment is created by rolling a rack on the pitch circle of the gear. Then, by axially shifting and rotating a 3-D helical tooth is generated. Finally, the complete gear is built as a circular pattern (Fig. 3).

Meshing. The mesh should be fine enough in order to account for the Hertzian footprint width and the deviations. Keep in mind that both are usually some orders of magnitude smaller than the overall teeth dimensions. Of course, it should be considered that the overall number of elements must be as low as possible. Therefore, the critical areas must be managed in a special way in order to obtain reasonable results. In the current model, there are two, i.e. — the first includes the contact lines defined by the intersections of the active flanks and the plane of action of the meshing gears; the second is defined by the root fillet of each tooth flank. The mesh is generated in two steps. At first, the surfaces defining the gears are meshed using triangular shell elements. Then, using them as reference, the volume mesh is generated using triangular elements. In order to define the abovementioned areas, so-called "refinement hexahedral boxes" (MORPHBOX) are used; surfaces inside them are meshed with different mesh parameters. The meshing procedure is automated using the mesh generator provided by the pre-processor (BATCH MESH). Since many snapshots need to be generated and solved, the process is fully automated using *Python* scripting.

In order to define the mesh parameters and quality criteria, a well-known model of cylinder-to-cylinder contact is solved and evaluated by the Hertzian theory; the model is presented in Figure 4. One hexahedral box was used in order to define the region of interest. Surfaces inside the box are meshed using the "solids structural mesh" algorithm with 0.04 target element length and allowable range 0.02 ... 0.5 mm. Transverse planes are meshed using the so-called "CFD" algorithm, which provides fast and smooth transition from fine to coarse mesh. The growth rate was set to 1.5 and the allowable range of the element length 0.03 ...0.5 mm. In all mesh algorithms, the minimum/maximum element angle was limited to 45^0 ...75^0.

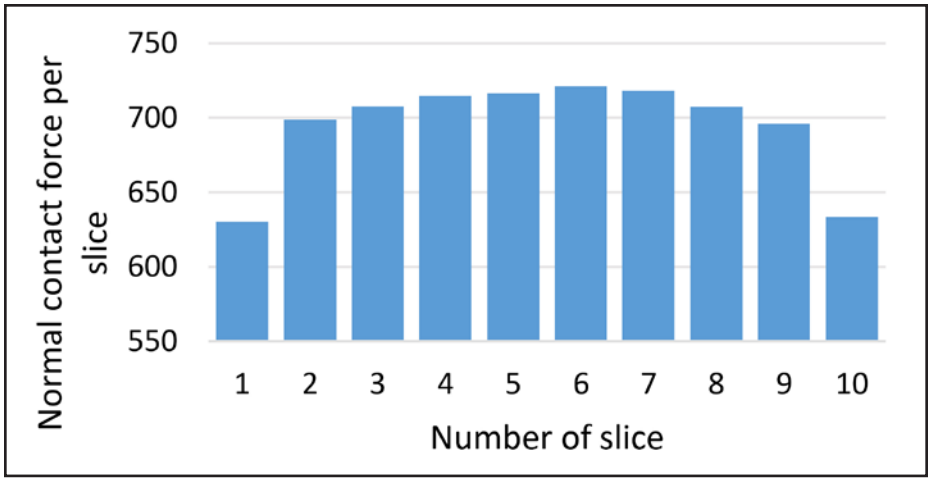

Figure 5 Contact normal forces distribution in cylinder.

The contact normal forces distribution is shown (Fig. 5). It is obvious that the resulting normal force per slice is smaller at the edges than in the middle of the width, because the stiffness is smaller there. According to the analytical solution, the mean value of contact force is almost 677 N-per-slice — which is well confirmed. Therefore, the abovementioned parameters are used in the next steps of the study.

Morphing. Morphing is a tool provided by *ANSA* and it allows for shape modifications that can be applied in both finite element model and geometry. Using morphing reduces the modeling time required because it helps to avoid going back in the geometry generation stage or even in CAD model. Usually, morphing is applied using boxes containing the geometry which will be modified. However, a special procedure called "direct morphing" is applied without morphing boxes. This can be performed either by specifying "frozen" areas and "morphing" zones, or by fitting the initial edges to target curves.

In the current case, "direct morphing" is used and specific boundaries are defined, regarding the geometry.

Pitch errors can be modeled as angular displacements of the active gear flanks. The displacement angle can be selected in such a way that the thickness of the tooth is changed at a chosen magnitude. In Figure 6 the affected surfaces are shown: 1 (green colored) is the morphing surface, 2 (purple colored) the affected surfaces and finally 3 (blue lines) the boundaries of the morphing action.

Boundary conditions. At first, modeling the shaft is ignored. Rather, the gears are modeled with a bore in the center. Torque is applied uniformly along the width on the inner surface of the pinion bore using multi-point constraints ("MPC", "RIGID" type). In this way, the deformation of the teeth is the only parameter affecting the load distribution.

The gear was considered fixed at the inner surface of its bore; Figure 7 shows the support of the pinion and the gear.

Next, the shaft's geometry is inserted in the model. As expected, the deformations of each shaft affect the load distribution and it needs to be considered. The shafts are supported by bearings; at one end by a locating bearing and at the other end a floating one. They are modeled using the "COUPLING" of "DISTRIBUTE" type of elements in order to have a statically well-defined model and allow the shafts to deform in the way they actually do. The bearings are considered very stiff compared to the gears, and they are not included in the model. In Figure 8 the gear pair including the shafts is shown.

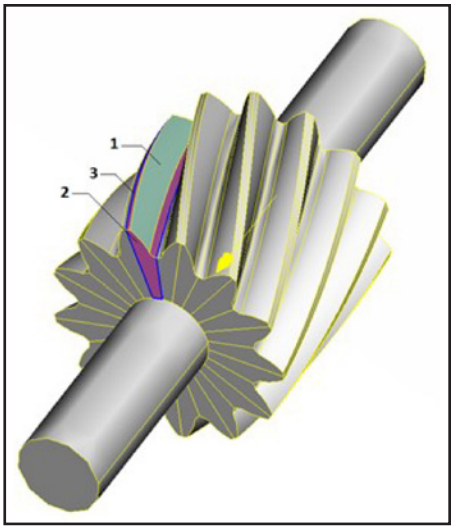

Figure 6 Surfaces used in morphing.

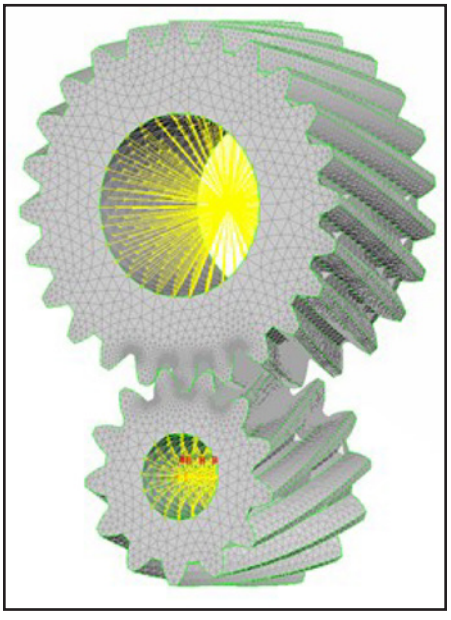

Figure 7 Members support modeling.

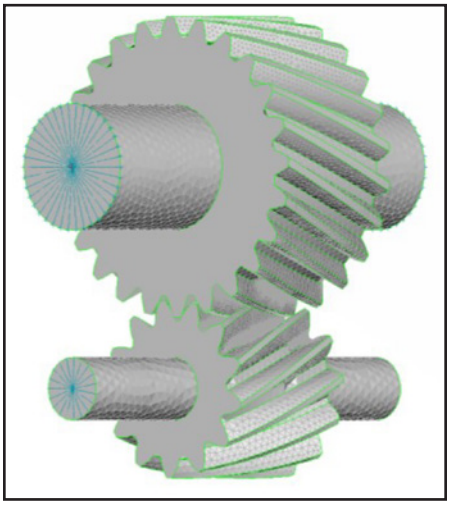

Figure 8 Gear pair including shafts.

Solution Scheme and Results

Figure 9 shows an overview of the solution scheme and the *Python* scripts developed.

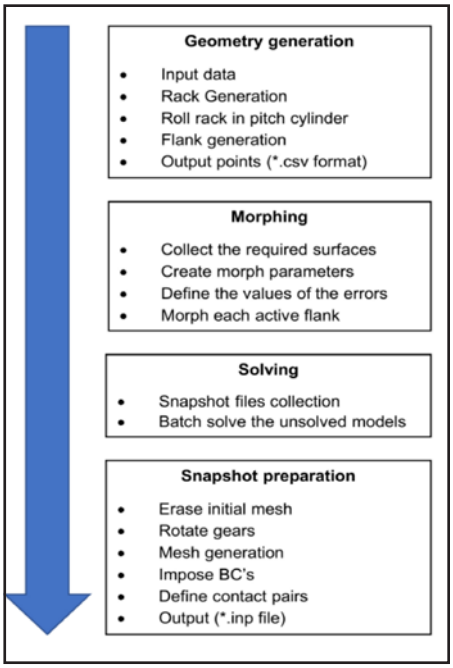

Figure 9 Overview of the Python scripts used.

position in order to emphasize the parameters that influence the load distribution. On the left-hand side, the resulting contact footprint is presented; on the right-hand side, the load distribution along the width is depicted; each gear is sliced per 1 mm.

At first, in spur gears (Case A, Fig. 10) the load distribution is uniform in both snapshots, as expected, because perfect geometry is assumed and only deformations of the teeth are considered. In the second snapshot, two gear pairs are in contact and the load is uniformly distributed along the face width of both.

Next, in helical gears (Case B, Figure 11), the contacting flanks are three because of the overlap ratio of helical gears. The load distribution along the lines of contact is almost uniform. The deviations occur from the varying curvature and stiffness. In both cases (A and B) only the deformation of the teeth is considered.

The deformation of the shafts is introduced in Case C, Figure 12. Compared with the previous case a slope in the load distribution is observed. Finally, Case D, Figure 13 demonstrates the profound impact of the pitch errors:

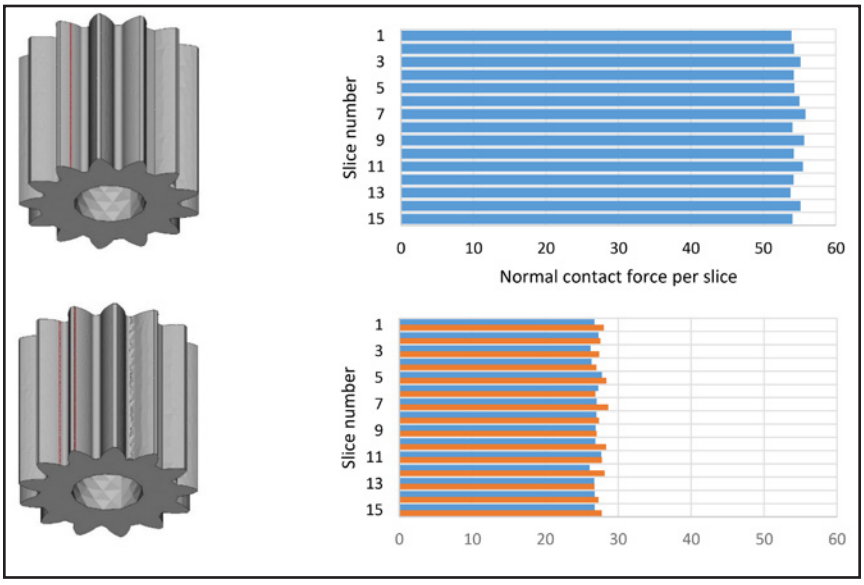

Figure 10 Case A results.

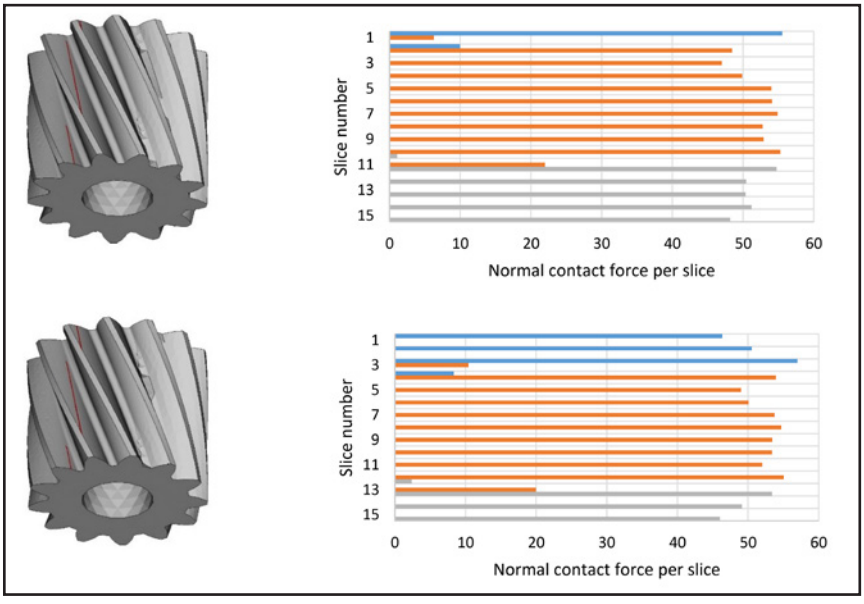

Figure 11 Case B results.

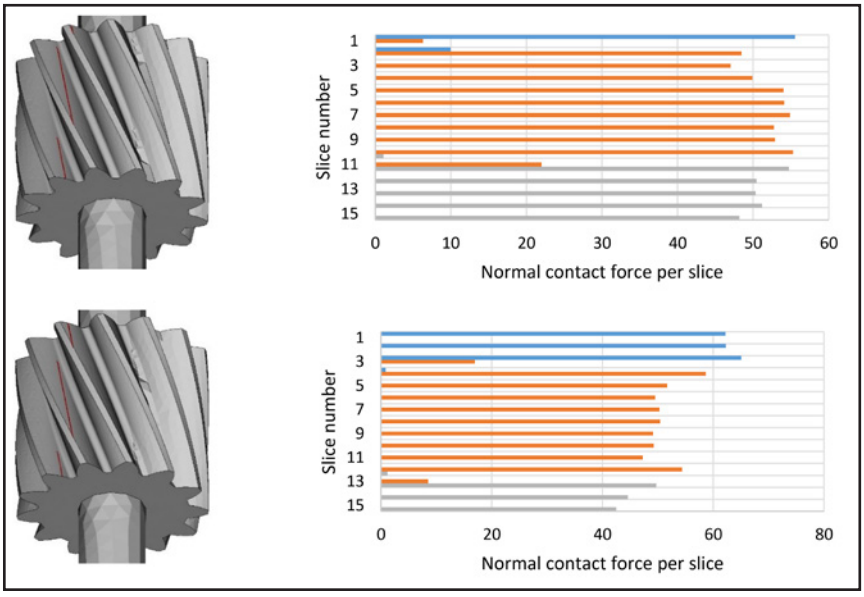

Figure 12 Case C results.

One active flank may contact and consequently transfer no load at all, resulting in increased loading on the rest of the active flanks.

Conclusions

The load distribution along the face width of spur gear pairs was analyzed in the current study. Both straight and helical geometries were considered. In order to define the mesh parameters, and the quality criteria, a simple model of two contacting parallel cylinders was made. The analysis used smart software techniques in order to keep the number of elements as low as possible. Also, extensive *Python* scripting was employed in order to accelerate recurrent tasks during the modeling procedure.

Results confirmed that load distribution is affected by the deformation of other members of the transmission besides the gear teeth. Furthermore, manufacturing deviations strongly affect the load distribution. In extreme cases, they can determine the actual number of active flanks. Next steps of the research may include a multi-snapshot analysis or the calculation of $K_{H\beta}$ coefficient. **PTE**

Acknowledgment. This project is supported by BETA CAE Systems, which provides the *ANSA* and *META* software.

For more information.

Questions or comments regarding this paper? Contact Prof. Athanassios Mihailidis at *amih@auth.gr*.

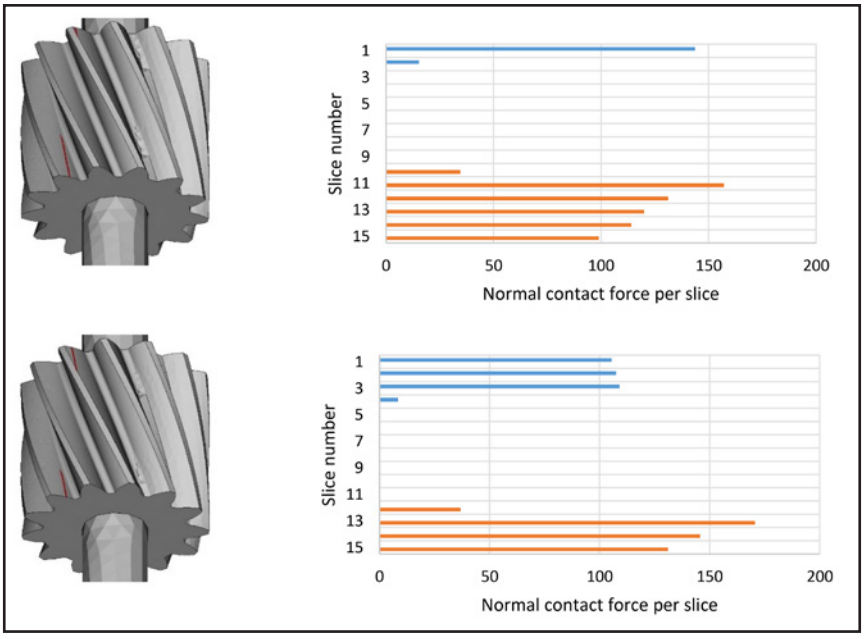

Figure 13 Case D results.

References

1. Zhou, C., C. Chen, L. Gui and Z. Fan. "A Nonlinear Multi-Point Meshing Model of Sur Gears for Determining the Face Load Fctor," *Mechanism and Machine Theory*, 126 (2018) 210–224.
2. Roda-Casanova, V., F. T. Sanchez-Marin, I. Gonzalez-Perez, J. L. Iserte and A. Fuentes. "Determination of the ISO Face Load Factor in Spur Gear Drives by the Finite Element Modeling of Gears and Shafts," *Mechanism and Machine Theory*, 65 (2013) 1–13.
3. Yuan, B., S. Chang, G. Liu, L. Chang and L. Liu. "Quasi-static Analysis Based on Generalized Loaded StaticTransmission Error and Dynamic Investigation of Wide-Faced Cylindrical Geared Rtor Stems," *Mechanism and Machine Theory*, 134 (2019) 74–94.
4. BETA CAE Systems S.A. *ANSA* version 19.1.3 User's Guide, 2019.
5. BETA CAE Systems S.A. *META* version 19.1.3 User's Guide, 2019.

Athanassios Mihailidis is Professor and Director of the Laboratory of Machine Elements & Machine Design of the School of Mechanical Engineering of the Aristotle University of Thessaloniki. His research interests include machine elements, gears and power transmission systems, tribology and thermo-elastohydrodynamic lubrication, as well as automotive engineering. Mihailidis is a founding member of the Balkan Tribological Association as well as of the Balkan Association of Power Transmissions.

Andreas Psarros studied mechanical engineering at the Aristotle University of Thessaloniki. Currently, he works as a Research Assistant in the Lab. of Machine Elements and Machine Design.Psarros's research interests include gears, planetary gearboxes and additive manufacturing — especially lattice structures and their properties for use in machine elements.